1-24-1994

Effect of Negative Ions on Electrical Breakdown in a Nonuniform Air Gap Between a Wire and a Plane

K. Ramakrishna
IBM Corporation

Ira M. Cohen
University of Pennsylvania

Portonovo S. Ayyaswamy
University of Pennsylvania, ayya@seas.upenn.edu

Effect of Negative Ions on Electrical Breakdown in a Nonuniform Air Gap Between a Wire and a Plane

Abstract
Electrical breakdown of an axisymmetric, atmospheric pressure air gap between a wire and a plane has been investigated for a gap length of 0.5 mm. 0^- and 0_2^- have been identified as the negative ions affecting the discharge development in air, besides electrons and positive ions, and have been included in the electrical breakdown model. Five coupled two-dimensional transient partial differential equations describing the discharge evolution in the air gap have been solved using a finite difference algorithm developed earlier. Temporal development of the charged particle number densities, electrostatic potential, electric field, and current at both the electrodes is presented when the wire is negatively biased at 2500 V. The impact of negative ions on gap breakdown has been assessed by comparing the results of analyses with and without negative ions. It is concluded that the negative ions have negligible effect during the early stages of the discharge development. However, as the discharge evolves, the negative ions cause a net loss of electrons from the discharge. The effect is most pronounced away from the discharge axis, where peaks in the electron density occur as breakdown proceeds. Radial spread of discharge and current growth rate are relatively unaffected by the presence of negative ions, but the magnitude of total current at the electrodes has been found to decrease by a decade when the negative ions are present.

Disciplines
Engineering | Mechanical Engineering

Comments
Suggested Citation:
Ramakrishna, K., Ira M. Cohen and Portonovo S. Ayyaswamy. (1994). *Effect of negative ions on electrical breakdown in a nonuniform air gap between a wire and a plane.* Physics of Plasmas. Vol. 1(5).

Effect of negative ions on electrical breakdown in a nonuniform air gap between a wire and a plane

K. Ramakrishna
Materials Science, Endicott Electronic Packaging, Microelectronics Division, IBM Corporation, Endicott, New York 13760-8000

I. M. Cohen and P. S. Ayyaswamy
Department of Mechanical Engineering and Applied Mechanics, University of Pennsylvania, Philadelphia, Pennsylvania 19104-6315

(Received 20 October 1993; accepted 25 January 1994)

Electrical breakdown of an axisymmetric, atmospheric pressure air gap between a wire and a plane has been investigated for a gap length of 0.5 mm. O^- and O_2^- have been identified as the negative ions affecting the discharge development in air, besides electrons and positive ions, and have been included in the electrical breakdown model. Five coupled two-dimensional transient partial differential equations describing the discharge evolution in the air gap have been solved using a finite difference algorithm developed earlier. Temporal development of the charged particle number densities, electrostatic potential, electric field, and current at both the electrodes is presented when the wire is negatively biased at 2500 V. The impact of negative ions on gap breakdown has been assessed by comparing the results of analyses with and without negative ions. It is concluded that the negative ions have negligible effect during the early stages of the discharge development. However, as the discharge evolves, the negative ions cause a net loss of electrons from the discharge. The effect is most pronounced away from the discharge axis, where peaks in the electron density occur as breakdown proceeds. Radial spread of discharge and current growth rate are relatively unaffected by the presence of negative ions, but the magnitude of total current at the electrodes has been found to decrease by a decade when the negative ions are present.

I. INTRODUCTION

Studies on initiation of electrical breakdown between a wire and planar electrode are of interest for a fundamental understanding of the phenomena involved. They are also encountered in industrial situations such as in microelectronic interconnection by the ball bonding process. Characteristics of electrical breakdown in a gas between two electrodes have been studied widely by assuming electrons and positive ions as the major charge carriers for plane parallel and nonuniform gap geometries.[1–5] Most of the analytical treatments of the subject have employed one-dimensional models for parallel plane geometry, and the resulting species conservation and electric field equations have been numerically solved by the method of characteristics.[6] A few two-dimensional analyses of breakdown between parallel planes are also available.[7–9] Until recently, studies addressing breakdown in nonuniform gaps have dealt with the axial development of the discharge, and the gap nonuniformity has been accounted for by its effect on the initial potential distribution in the gap.[10,11] Complete two-dimensional analyses of discharge initiation in a nonuniform gap between a hyperboloidal wire and a plane have been solved for initial breakdown[12–13] and have been extended to the formation of a quasineutral region in the gap.[14] Jog, Cohen, and Ayyaswamy[15,16] have included the effects of electron and ion temperature evolution on the breakdown characteristics in such gaps by adding particle energy equations to the prior isothermal formulations describing breakdown of the gas. Assuming that the discharge would evolve into an arc discharge eventually (for long times), Vacek and Cohen[17] have solved a semiempirical model to determine transient temperature and heat transfer to the wire and electric field in the gap. Analytical and experimental investigations of breakdown phenomena in nonuniform gaps are reviewed in Refs. 18–21.

Studies of electrical breakdown of gases with electrons and positive ions as the sole charge carriers provide generic descriptions of events occurring during the breakdown process. However, in electronegative gases, like air and oxygen, experimental evidence points to the formation of negative ions. As the formation and destruction of negative ions involves the electrons, the negative ions can cause net loss or gain of the electrons in regions of the discharge. On the other hand, unstable negative ions give up electrons, which reenter the discharge and contribute to ionization and breakdown processes; electrons gained by the stable negative ions are permanently lost from the discharge. Thus, the negative ions are expected to play an important role in the events occurring during electrical breakdown of the gases.

Very few studies dealing with the effect of negative ions on discharge development in air have been reported in the literature.[22,23] These studies have employed one-dimensional approximations in parallel plate geometry and accounted for the presence of O^- and O_2^- in their models. In these studies, the effects of photoemission on the discharge development have also been accounted for. They have concluded that the negative ions hinder the growth

 1070-664X/94/1(5)/1349/10/$6.00

TABLE I. Reactions involving negative ions of oxygen in air.

Mechanism	Reaction	Remarks
Associative attachment	$O_2+e\rightarrow O_2^-$	For $p<1000$ Torr, $\alpha_{aa}=0$.
Direct impact attachment[26] (three-body)	$2O_2+e\rightarrow O_2^-+O_2$	Reaction occurs for $E'/p<2$ V/Torr cm. Does not contribute to negative ion formation at higher values of E'/p.
Dissociation into ions[33]	$2O_2+2e\rightarrow O_2^++2O^-+e$	Reaction requires high-energy electrons ($\sim$17.1 eV).
Three-body process[26]	$O_2^-+O_2\rightarrow O_3^-+O$	Rate constant is negligibly small compared to other reactions. Occurs when $2<E'/p<10$ V/Torr cm.
Dissociative attachment[26]	$O_2+e\rightarrow O_2^-{}^*\rightarrow O^-+O$	Unstable O^- negative ions form during this process.
Electron detachment[26]	O^-+O_2 (or N_2) $\rightarrow O_2$ (or N_2) $+O+e$	
Charge transfer[26]	$O^-+O_2\rightarrow O_2^-+O$	Stable O_2^- ions are formed.

rate of current with the maximum decrease occurring when unstable ions are present.

A two-dimensional analysis[12] of discharge breakdown in a nonuniform gap between a wire and a plane has shown that as the discharge develops, the electron density maximum moves away from the discharge axis when the wire is negatively biased with respect to the plane. Since the production and loss of negative ions depend on the local electron density, the role of negative ions is expected to be more complex in a nonuniform gap than in a parallel plate uniform gap.

In this paper, the effect of negative ions on the discharge breakdown in a nonuniform gap between a wire and a plane is studied by employing a two-dimensional form of diffusion flux equations when electrons, positive ions, and O^- and O_2^- negative ions are the charge carriers. Equations governing the charged particle densities and electrostatic potential in a nonuniform air gap have been solved by a finite difference method for a gap length of 0.5 mm when the wire is negatively biased with respect to the plane for an applied potential difference of 2500 V.

II. IDENTIFICATION OF THE REACTIONS PRODUCING THE NEGATIVE IONS

Electronegative gases, such as air and oxygen, gain electrons, and the resultant system is at an energy level lower than the ground level of the neutral molecule. The difference in energy between the ground state and the negative ion is released in several ways, resulting in such processes as radiative attachment, dissociative attachment, three-body attachment, and dissociation into ions. Both stable and unstable negative ions are formed in electronegative gases. A stable negative ion (for example, O_2^-) retains the electron gained during the attachment process and an unstable negative ion (like O^-) gives it up either in a detachment process or transfers it to another neutral in a charge transfer process. Reactions involved in the production and loss of negative ions in air are summarized in Table I.

Comprehensive reviews by Dutton[24] and Gallagher *et al.*[25] also concur that the reactions summarized above accurately describe the formation of negative ions in air. A spectroscopic study by Moruzzi and Phelps[26] has concluded that negative ions of nitrogen do not form in pure nitrogen or in nitrogen–oxygen mixtures. Table II summarizes the reactions that produce negative ions with major impact on discharge development in air at atmospheric pressure.

III. DEVELOPMENT OF THE MODEL

We now consider a slightly ionized, collision-dominated plasma which is adequately described by the continuum (diffusion flux) conservation equations. The diffusion flux equations are given by:[27,28]

TABLE II. Reactions used in the modeling of discharge breakdown in atmospheric pressure air.

Mechanism	Reaction	Remarks
Electron-impact ionization	O_2 (or N_2) $+e\rightarrow O_2^+$ (or N_2^+) $+2e$	Produces electrons and positive ions
Dissociative attachment	$O_2+e\rightarrow O_2^-{}^*\rightarrow O^-+O$	Forms O^- ions. Electrons are lost from the discharge region.
Electron detachment	O^-+O_2 (or N_2) $\rightarrow O_2$ (or N_2) $+O$	Loss of O^- from the discharge and gain of electrons.
Charge transfer	$O^-+O_2\rightarrow O_2^-+O$	Source of stable O_2^-.

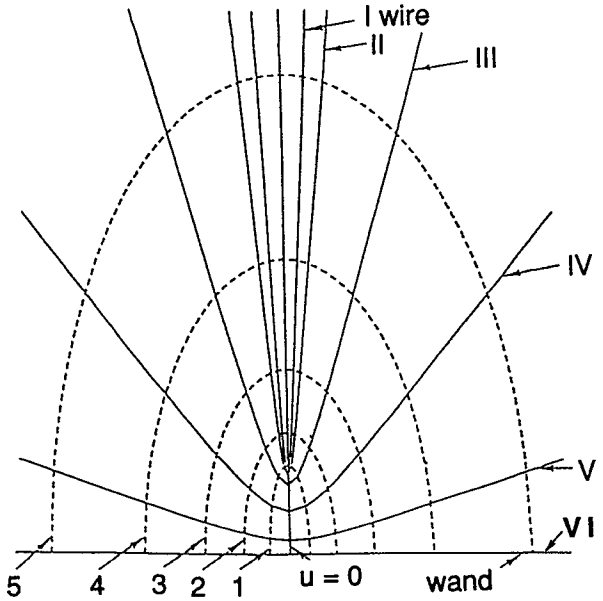

FIG. 1. Schematic diagram of prolate spheroidal coordinate system for the study of electrical breakdown between a wire and a plane. Legend: (1) $u=0.5$; (2) $u=1.0$; (3) $u=1.5$; (4) $u=2.0$; (5) $u=2.5$. (I) $v=0.1$; (II) $v=0.1785$; (III) $v=0.5$; (IV) $v=1.0$; (V) $v=1.4$; (VI) $v=\pi/2$ (plane).

$$\frac{\partial N_+}{\partial t'}+\nabla'\cdot\Gamma'_+=P(N_+)-R(N_+) \quad \text{for positive ions,} \tag{1}$$

$$\frac{\partial N_e}{\partial t'}+\nabla'\cdot\Gamma'_e=P(N_e)-R(N_e) \quad \text{for electrons,} \tag{2}$$

$$\frac{\partial N_{O^-}}{\partial t'}+\nabla'\cdot\Gamma'_{O^-}=P(N_{O^-})-R(N_{O^-}) \quad \text{for } O^- \text{ ions,} \tag{3}$$

$$\frac{\partial N_{O_2^-}}{\partial t'}+\nabla'\cdot\Gamma'_{O_2^-}=P(N_{O_2^-})-R(N_{O_2^-}) \quad \text{for } O_2^- \text{ ions,} \tag{4}$$

$$\nabla'\cdot\mathbf{E}'=\frac{e}{\epsilon_0}(N_+-N_{O^-}-N_{O_2^-}-N_e), \tag{5}$$

where,

$$\Gamma'=-D\nabla' N\pm\mu N\mathbf{E}', \tag{6}$$

where N is the number density, P is the production (ionization) rate, R is the recombination rate, Γ' is particle current density such that

$$I'=e\int_S[\Gamma'_+-\Gamma'_{O^-}-\Gamma'_{O_2^-}-\Gamma'_e]\cdot d\mathbf{S} \tag{7}$$

is the current passed by the discharge, D's are the diffusion coefficients, μ's the mobilities, and $\mathbf{E}'$ the self-consistent electric field.

It is appropriate to use prolate spheroidal coordinates to solve this problem (refer to Fig. 1).[29] In these coordinates, the wire electrode corresponds to $v=v_w$, which is nonzero and needs to be specified, and the wand to $v=\pi/2$. $u=0$ is the centerline of the discharge and $u\to\infty$ is into the ambient.

Boundary conditions:

$$\text{on } v=v_w,\quad V=V_w,\quad N_+=N_e=N_0,\quad N_{O^-}=N_{O_2^-}=0, \tag{8a}$$

$$\text{on } v=\pi/2,\quad V=0,\quad N_+=N_e=N_0,\quad N_{O^-}=N_{O_2^-}=0, \tag{8b}$$

$$\text{on } u=0,\quad \frac{\partial V}{\partial u}=0=\left.\frac{\partial N}{\partial u}\right|_{+,e,O^-,O_2^-}\to\text{symmetry condition,} \tag{8c}$$

and

$$\text{as } u\to\infty,\quad \frac{\partial V}{\partial u}\to 0,\quad \left.\frac{\partial N}{\partial u}\right|_{+,e,O^-,O_2^-}\to 0. \tag{8d}$$

Initial conditions: The number density of electrons and ions, N_0, is nonzero due to the omnipresent background radiation and has a value of 6×10^8 m^{-3} (Fleagle and Businger[30]), and the number densities of negative ions are zero at the beginning of the breakdown process. The initial potential distribution is given by the solution to Laplace's equation in prolate spheroidal coordinates (Ref. 13, pp. 165–167):

$$V=\frac{V_w\ln[\tan(v/2)]}{\ln[\tan(v_w/2)]}. \tag{9}$$

In order to complete the formulation of the problem, charged particle production and loss mechanisms have to be quantified.

A. Modeling of ionization and recombination mechanisms

Basic mechanisms for the production and loss of positive ions and electrons are discussed by Ramakrishna, Cohen, and Ayyaswamy.[12] With the inclusion of negative ions in the model, the loss (due to attachment) and gain (due to detachment) of electrons are also accounted for in the electron conservation equation. The net volumetric rate of production of the particles is given by the following:

(a) Positive ions, including impact and thermal ionization:

$$P_+|_{\text{impact and thermal ionization}}=\alpha_i\mu_e N_e E'+\gamma_e(T'_e)N_e\times(N^2_{\text{Saha}}-N_eN_+); \tag{10}$$

(b) Electrons, including impact and thermal ionization:

$$(P_e-R_e)|_{\text{impact, thermal ionization, attachment and detachment}}=\alpha_i\mu_e N_e E'+\gamma_e(T'_e)N_e(N^2_{\text{Saha}}-N_eN_+)-\alpha_{ad}\mu_e E'N_e+\alpha_d\mu_{O^-}E'N_{O^-}; \tag{11}$$

(c) O^- ions:

$$(P_{O^-} - R_{O^-})\,|_{\text{attachment, detachment, and charge transfer}}$$
$$= \alpha_{ad}\mu_e E' N_e - \alpha_d \mu_{O^-} E' N_{O^-} - \alpha_{ct}\mu_{O^-} E' N_{O^-}; \quad (12)$$

(d) O_2^- ions:

$$P_{O_2^-}\,|_{\text{charge transfer}} = \alpha_{ct}\mu_{O^-} E' N_{O^-}. \quad (13)$$

B. Rate coefficients for the negative-ion formation

The coefficients (α's) used in the characterization of various production and loss rates involving the negative ions depend upon the magnitude of the local electric field and the gas pressure as a ratio, E'/p, without additional dependence on pressure.[26,31] A brief review of the literature pertaining to the determination of these coefficients now follows.

From their experimental data in air (11–40 Torr) and oxygen (40–80 Torr) Harrison and Geballe[32] have calculated direct and dissociative electron attachment coefficients in prebreakdown discharges in which the secondary processes do not influence the discharge structure. The negative ions have been treated generically. Prasad[31] has extended the pressure range to 60–700 Torr for these coefficients and investigated dry air. The agreement with the values reported by him and Harrison and Geballe[32] is not good. Both of these investigations do not consider the effect of electron detachment on their experimental conditions. The studies of Prasad and Craggs,[33] Sukhum, Prasad, and Craggs,[34] Eccles and Craggs,[35] Daniel, Dutton, and Harris,[36] and Wagner[37] are concerned with the formation of unstable negative ions, which are destroyed through electron detachment or charge transfer. The experimental measurements of Moruzzi and Price[38] in dry air do not show any effects of attachment processes, and they suggest that a fast detachment process involving excited states of nitrogen may be operative. This study indicates that the negative ions may not influence the spatial growth of the discharge in air. The spatial growth experiments of Dutton, Llewellyn-Jones, and Palmer[39] in dry air in the pressure range 400–1000 Torr show that the ratio of attachment coefficient to gas pressure, at high pressures, depends solely on the ratio E'/p and that any additional dependence on pressure can be neglected. Wagner[37] has presented a detailed analysis of all the data then available to evaluate the attachment, detachment, and charge transfer coefficients in air and oxygen. Gallagher *et al.*[25] have critically reviewed the electron swarm data of electronegative gases (including air and oxygen) and updated the earlier compilation by Dutton.[24] From this review, it appears that the data of Wagner[37] are the most recent and accurate for negative-ion processes in air and it is used in this analysis.

Based on these data, the dependence of the coefficients for negative-ion formation on E'/p is derived:

$$\alpha_{ad}/p = A_{ad}(m/N), \quad (14)$$

$$\alpha_d/p = A_d e^{-B'_d p/E'}(m/N), \quad (15)$$

$$\alpha_{ct}/p = A_{ct}|E'/p - (E'/p)_{0,ct}|H((E'/p) - (E'/p)_{0,ct})(m/N), \quad (16)$$

where the subscripts 0,ct denote the threshold value of E'/p below which charge transfer does not occur. From Wagner's[37] data, $(E'/p)_{0,ct}$ is determined to be 2.28×10^6 V/mTorr. In the above equations $H(E' - E'_0)$ is the Heaviside function. It has a value of unity for $E' > E'_0$ and zero for $E' < E'_0$.

Constants in Eqs. (12)–(14) are determined by curve fitting the numerical data in Wagner[37] and are $A_{ad}=0.012$ m/N, $A_d=539$ m/N, $B'_d = 215.6$ m/N, and $A_{ct}=0.042$ 1/V. The range of E'/p for this data is 25–50 V m/N. For lack of data in the range of interest to this study (400–8000 V/cm Torr), it is assumed that the coefficients based on Wagner's data remain valid for describing the reactions modeled in this study (Sec. III A). The coefficients for impact ionization are discussed in Refs. 3 and 9. The mobility of O^- ions is taken to be 4.92×10^{-4} m^2/(V s) and that of O_2^- ions as 2.46×10^{-4} m^2/(V s) (Brown[40]). The mobility of O_2^- ions is taken to be equal to that of molecular oxygen, and the mobility of O^- ions is estimated from molecular oxygen in proportion to its mass.

C. Species conservation equations

The charged particle conservation equations can now be written as follows.

(a) Positive ions:

$$\frac{\partial N_+}{\partial t'} - \nabla'\cdot(\mu_+ N_+ \nabla' V) - \nabla'\cdot(D_+ \nabla' N_+)$$
$$= A_i p \mu_e E' N_e e^{-B'_i p/E'} + 1.09\times10^{-20} N_e T'^{-9/2}_e \times \left[\frac{2g_i N_n}{g_n}\left(\frac{2\pi m_e k T'_e}{h^2}\right)^{3/2} e^{-eV_i/kT'_e} - N_e N_+\right]. \quad (17)$$

(b) Electrons: In the presence of negative ions, electrons are additionally lost due to the attachment process, but they reenter the discharge due to the detachment process. The last two terms on the right-hand side of Eq. (18) reflect this:

$$\frac{\partial N_e}{\partial t'} + \nabla'\cdot(\mu_e N_e \nabla' V) - \nabla'\cdot(D_e \nabla' N_e)$$
$$= A_i p e^{-B'_i p/E'} \mu_e E' N_e + 1.09\times10^{-20} N_e T'^{-9/2}_e \times \left[\frac{2g_i N_n}{g_n}\left(\frac{2\pi m_e k T'_e}{h^2}\right)^{3/2} e^{-eV_i/kT'_e} - N_e N_+\right] - A_{ad} p \mu_e E' N_e + A_d p e^{-B'_d p/E'} \mu_{O^-} E' N_{O^-}. \quad (18)$$

(c) O^- ions:

$$\frac{\partial N_{O^-}}{\partial t'} + \nabla'\cdot(\mu_{O^-} N_{O^-} \nabla' V) - \nabla'\cdot(D_{O^-} \nabla' N_{O^-})$$
$$= A_{ad} p \mu_e E' N_e - A_d p \mu_{O^-} N_{O^-} E' e^{-B'_d p/E'} - A_{ct} p N_{O^-} E' |E'/p - (E'/p)_{0,ct}| H(E' - E'_{0,ct}). \quad (19)$$

(d) O_2^- ions:

$$\frac{\partial N_{O_2^-}}{\partial t'}+\nabla'\cdot(\mu_{O_2^-}N_{O_2^-}\nabla' V)-\nabla'\cdot(D_{O_2^-}\nabla' N_{O_2^-})$$
$$=A_{ct}\,pN_O-E'\,|(E'/p)-(E'/p)_{0,ct}|\,H(E'-E'_{0,ct}). \tag{20}$$

The ion and electron temperatures are taken to be specified as constant and can be different. Negative- and positive-ion temperatures are assumed to be equal.

The above set of equations has been nondimensionalized (Ramakrishna, Cohen, and Ayyaswamy[12]) and a brief summary is provided. The following nondimensional quantities are defined:

$$n=N/N_R,\ \psi=V/V_R,\ E=E'/E'_R,$$
$$T=T'/T_\infty,\ t=t'/t'_R, \tag{21}$$

where

$$N_R=\frac{kT_\infty\epsilon_0}{e^2d^2},\ V_R=\frac{kT_\infty}{e},\ E'_R=\frac{V_R}{d},\ t'_R=\frac{1}{A_ip\mu_eE'_R}. \tag{22}$$

In the above equations, e is magnitude of electrical charge on a single electron, k is the Boltzmann constant, ϵ_0 is the permittivity of free space, A_i is the constant in the equation relating Townsend's first ionization coefficient to the ratio E'/p, d is twice the radius of curvature of the wire at its tip, and T_∞ is ambient temperature; t'_R is on the order of nanoseconds. Governing equations in nondimensional form are presented in Appendix B.

D. Numerical solution

Five simultaneous, time-dependent, second-order, nonlinear partial differential equations governing the discharge breakdown in a nonuniform gap are solved using a finite difference algorithm by Ramakrishna and co-workers.[13,41] Salient features of this algorithm are

(1) implicit time integration,
(2) central differences for discretization of diffusion terms,
(3) upwind difference method for the drift terms, and
(4) where possible, the ionization and recombination terms are linearized with a negative slope to satisfy the "positive coefficient rule" (Patankar,[42] p. 38).

Discretization of the partial differential equations results in simultaneous algebraic equations. The presence of far diagonal terms, the nonlinear nature of the ionization and recombination terms, and the coupling of the species conservation equations with Poisson's equation necessitate an iterative solution of the algebraic equations. A two-tier iteration scheme is used to solve the algebraic equations.[41] In this iterative scheme, with a guessed potential distribution, convergence on the number densities is first obtained at time $t+\Delta t$ [level $(l+1)$]. With these converged number density distributions, the potential distribution is updated by solving Poisson's equation. The current potential distribution is then employed in recalculating the number densities. This procedure is continued until the number densities and the potential are consistent with each other. Then, we advance to the next time level, viz., $l+2$. The first iteration begins with known solution at time t (level l). It was found useful to solve equations of electrons, positive ions, and O^- and O_2^- ions in an order in which they influence the breakdown characteristics, in the first tier. Alternatively, a three-tier system consisting of electrons and positive ions in the first tier, negative ions in the second, and the electrostatic potential in the third could have been employed. Convergence criteria, a flow chart, and the numerical experimentation are discussed in detail by Ramakrishna and co-workers.[13,41]

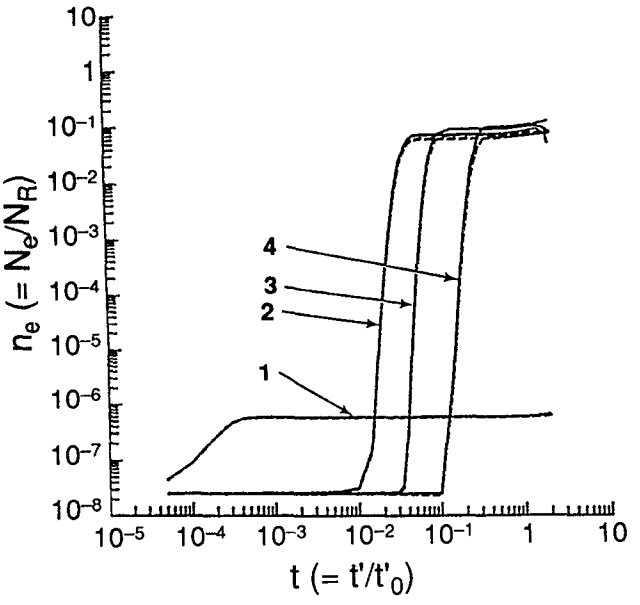

FIG. 2. Temporal development of the electron number density in air with and without negative ions. The wire is at −2500 V. Spatial locations on the discharge axis. $p=760$ Torr, $L=0.5$ mm, and $d=0.01$ mm. Legend: solid lines, without negative ions; dashed lines, with negative ions; (1) $Z=0.99$; (2) $Z=0.80$; (3) $Z=0.67$; (4) $Z=0.36$. (Z is fraction of axial distance from plane to wire tip.)

IV. RESULTS AND DISCUSSION

The normalized equations are solved for a negatively biased wire at a potential difference of 2500 V. The ambient pressure and temperature are 1 atm and 500 K, respectively. The electron temperature T'_e is fixed at 5000 K. The temperature of the heavy particles is taken equal to ambient temperature. A gap length of 0.5 mm (20 mils) and $v_w=0.1$ have been used in all of the computations. The diameter of the wire is taken to be twice the radius of curvature of the hyperboloid of revolution with $v_w=0.1$ and has a value of 0.01 mm. These geometric parameters are typical of the ball bonding process used in microelectronic interconnection. The initial density of the electrons and ions is taken to be 6×10^8 m^{-3} (Fleagle and Businger[30]). For these conditions, $N_R=2.36\times10^{16}$ m^{-3}.

Figure 2 shows temporal variation of the electron

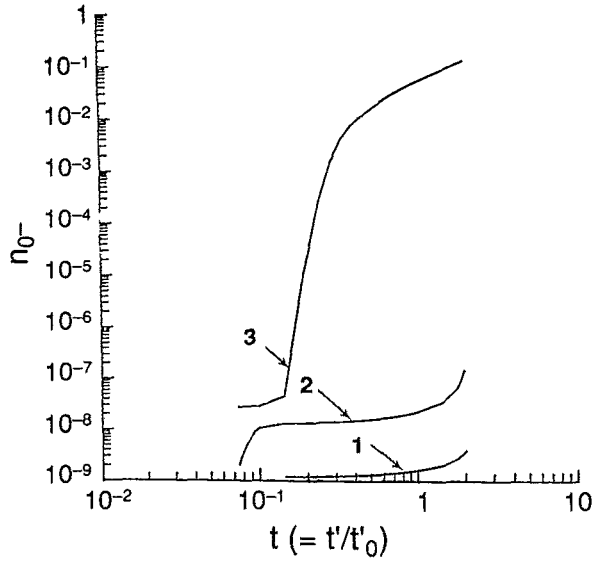

FIG. 3. Temporal development of number densities of negative ions of oxygen (O^-) in air at several points on the discharge axis with the wire at -2500 V. $p=760$ Torr, $L=0.5$ mm, and $d=0.01$ mm. Legend: (1) $Z=0.80$; (2) $Z=0.67$; (3) $Z=0.36$.

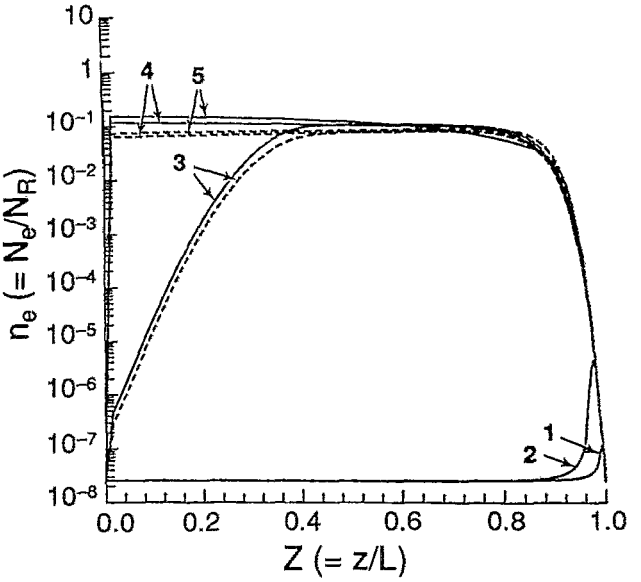

FIG. 5. Profiles of number densities of electrons in air on the discharge axis with and without negative ions. The wire is at -2500 V. $p=760$ Torr, $L=0.5$ mm, and $d=0.01$ mm. Legend: solid lines, without negative ions; dashed lines, with negative ions; (1) $t=10^{-4}$; (2) $t=7.5\times10^{-4}$; (3) $t=0.295$; (4) $t=0.795$; (5) $t=1.84$.

number densities at several locations on the discharge axis. The growth curves are compared to the growth curves obtained without the negative ions (from Ramakrishna and co-workers[12,13]). These growth curves indicate that the agreement between the two models (with and without negative ions) is good. The electron loss or gain appears to be too small to affect the growth of the discharge on the axis. The growth curves for the densities of the negative ions on the discharge axis are shown in Figs. 3 and 4 for O^- and O_2^-, respectively. These curves show that the densities of negative ions rise rapidly by several decades in a short time. However, the rise in density is less rapid than it is for the electrons at locations near the plane. The rise in negative-ion density occurs after the ionization wave (traveling due to impact ionization near the wire tip region) passes a given location.

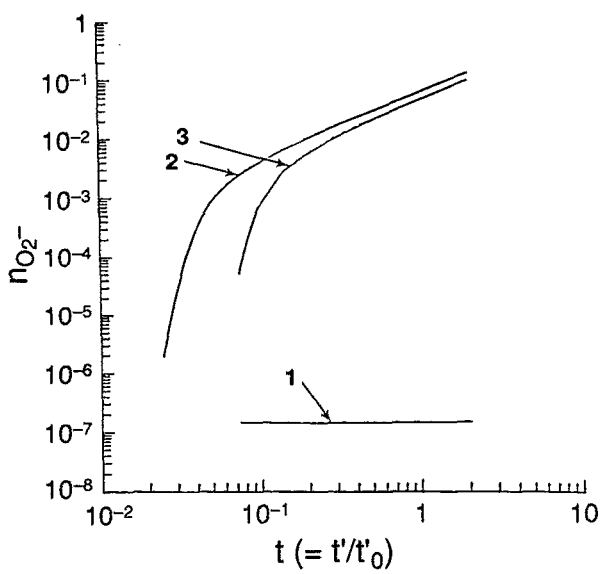

FIG. 4. Temporal development of number densities of negative ions of oxygen (O_2^-) in air at several points on the discharge axis with the wire at -2500 V. $p=760$ Torr, $L=0.5$ mm, and $d=0.01$ mm. Legend: (1) $Z=0.99$; (2) $Z=0.80$; (3) $Z=0.67$.

The axial number density profiles of the electrons at various stages of the breakdown are shown, with and without negative ions, in Fig. 5. This comparison shows that the effects of negative ions very early in the breakdown are negligible ($t\leqslant7.5\times10^{-4}$ in Fig. 4). At later times ($t\geqslant0.295$ in Fig. 5), the electron density is lower when the negative ions are present, and the lower density represents the net electron loss from the discharge. At $t=1.84$ the electron density without negative ions is nearly twice as much as the electron density with negative ions. Near the wire and at $t=1.84$, it is $0.075N_R$ with negative ions and $0.156N_R$ without negative ions.

Figure 6 shows axial profiles of O^- ions at various times during breakdown. These profiles show that the net production of the O^- negative ions occurs between the wire and the center of the discharge ($Z<0.8$). In this region the electron density and the electric field are very high and the attachment process is effective in producing the O^- ions. Near the plane the density of this specie of negative ion is nearly zero as the production rates are small due to small electron current.

The effect of negative ions on radial profiles of electrons is shown in Fig. 7 for a location near the wire ($Z=0.99$), where the electric field is very high. It may be

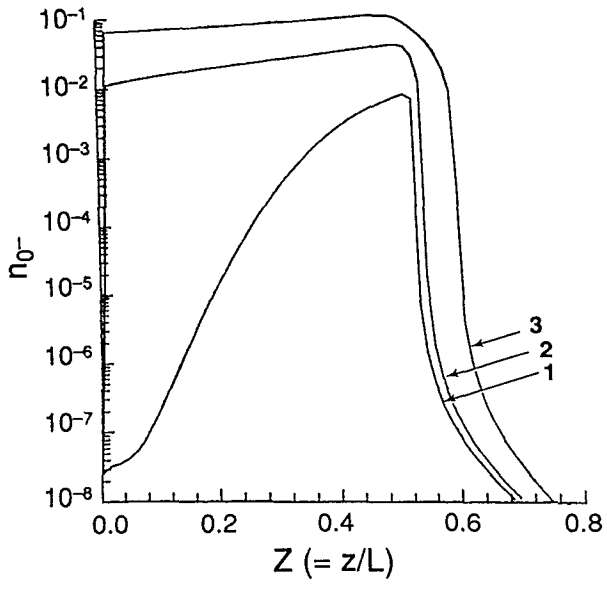

FIG. 6. Profiles of number densities of O^- ions in air on the discharge axis. The wire is at -2500 V. $p=760$ Torr, $L=0.5$ mm, and $d=0.01$ mm. Legend: (1) $t=0.295$; (2) $t=0.795$; (3) $t=1.84$.

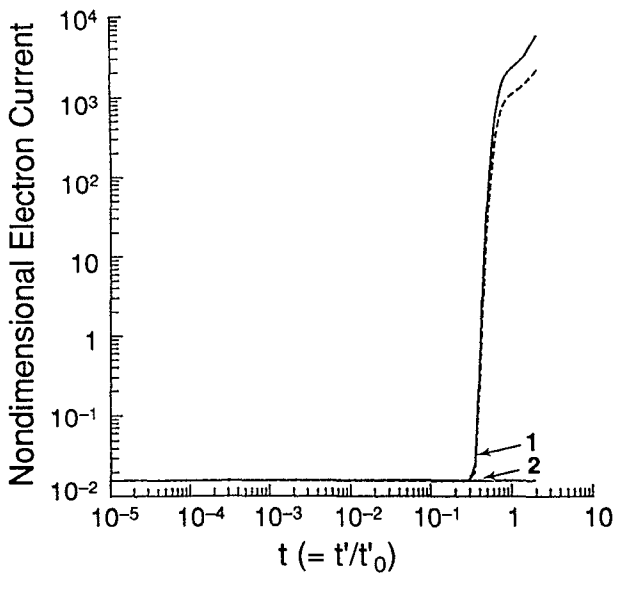

FIG. 8. Nondimensional electron current at the wire and at the planar electrode with and without negative ions in air. The wire is at -2500 V. $p=760$ Torr, $L=0.5$ mm, and $d=0.01$ mm. Normalization current is 2.8×10^{-9} A. Legend: solid lines, without negative ions; dashed lines, with negative ions; (1) at wire; (2) at planar electrode.

noted that the maximum values of electron and ion number densities occur on the discharge axis, $r=0$, at initial times, and as the breakdown progresses the peaks in radial number density profiles move off the discharge axis.[12,13] When the wire is negative, the radial component of the electric field, $E_r=-\partial\psi/\partial r$, is directed towards the axis, i.e., it is radially inward. As the electrons drift in a direction opposite to the local electric field, they move away from the axis at a rate proportional to the product n_eE_r. Initially n_e and the drift flux are small and the peaks occur on the axis. As time progresses, at any fixed location, the electron number density increases due to an increase in drift flux and volumetric production by impact ionization. We note also that densities are depressed very close to the wire because of the absorbing wall boundary condition. This requires the diffusive flux to dominate over the drift at the wall. These factors contribute to the electron number density peak occurring away from the axis as time increases, when the wire is negative. The electrons that drift away from the discharge axis cause ionization after sufficient buildup of their number density away from the axis. This is necessary as the electric field decreases radially outward and the local volumetric ionization rate is proportional to the product n_eE. The peak in the radial ion number density profile also occurs off the axis, when the wire is negative, as the production of ions depends upon the local electron density. Even though the ion drift is towards the axis, the ion number density still peaks away from the axis as the ion drift is much slower than the electron drift. It is seen here that the ion peaks shift slightly towards the discharge axis and electron peaks away from it. Figure 7 also shows that the electron density decreases in the presence of negative ions and the effect is most pronounced at later times ($t=1.84$). Near its peak, the electron density decreases by nearly two decades because of the negative ions. However, the peaks occur away from the axis for the negative polarity of the wire as breakdown progresses. The spread of the discharge

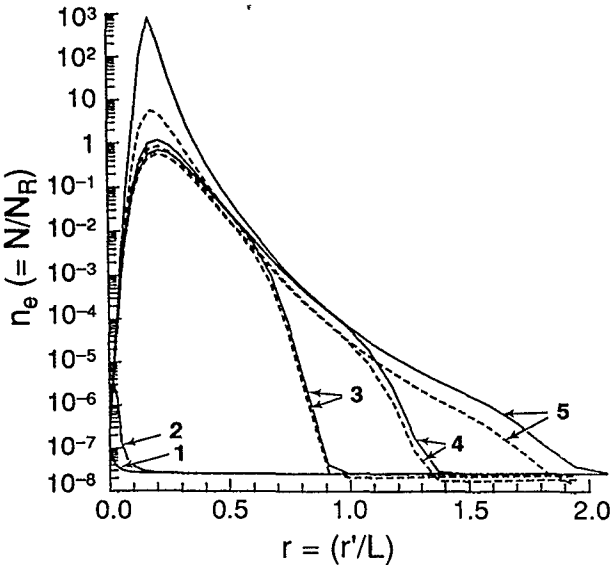

FIG. 7. Evolution of radial profiles of electron number density near the tip of the negatively biased wire with and without negative ions in the discharge. The wire is at -2500 V. $p=760$ Torr, $L=0.5$ mm, $d=0.01$ mm, and $Z=0.99$. Legend: solid lines, without negative ions; dashed lines, with negative ions; (1) $t=10^{-4}$; (2) $t=7.5\times10^{-4}$; (3) $t=0.295$; (4) $t=0.795$; (5) $t=1.84$.

is nearly the same—approximately two times the gap length.

Figure 8 shows current growth curves with and without negative ions. The normalization current is 2.8×10^{-9} A. The current rise occurs at the same time in both cases. When negative ions are present, the resulting current is about four times smaller because the negative ions cause loss of electrons from the discharge and the current rise is less rapid in the presence of negative ions.

V. SUMMARY AND CONCLUSIONS

In this paper, the breakdown characteristics of air in a nonuniform gap between a wire and a plane are studied by accounting for the formation of negative ions of oxygen through attachment, detachment, and charge transfer processes. The gap length is 0.5 mm and the applied voltage is -2500 V. The wire is biased negative with respect to the plane. It is found that the effect of the negative ions is negligible during the early phases of the breakdown and, at later times, the negative ions cause a net loss of electrons from the discharge. This effect is most pronounced away from the discharge axis, where the peaks in the electron density occur. The radial spread of the discharge is relatively unaffected by the presence of the negative ions. The current rise is also unaffected by the negative ions and the current levels are lower, by a decade, when the negative ions are present.

ACKNOWLEDGMENTS

The authors are grateful to Professor J. Dutton of the University of Swansea, U.K. and Professor Eric E. Kunhardt of the Weber Research Institute, Polytechnic University, Brooklyn, NY for many helpful discussions and encouragement.

This material is based upon work supported by the National Science Foundation under Grants Nos. DMC 8513128 and ENG 7825899. Numerical computations have been performed on the Cray X/MP-48 Supercomputer at the Pittsburgh Supercomputer Center under NSF Supercomputer Grant Nos. DMC 0000000/8513128 and ECS-8515068.

APPENDIX A: NOMENCLATURE

a: semifocal distance (m)
A: constant in the equation relating ionization coefficient to the ratio E'/p (m/N)
B_i': constant in the equation relating Townsend's first ionization coefficient to the ratio E'/p (m/N)
B_i: nondimensional form of B_i ($= B_i p/E_R'$)
C_1: constant in Eq. (B1)
C_2: constant in Eq. (B1)
d: twice the radius of curvature at the tip of the hyperboloidal wire (m)
$\mathbf{E}'$: dimensional electric field intensity (V/m)
$\mathbf{E}$: dimensionless electric field intensity
e: charge on a single electron (C)
F: a dimensionless parameter in Eqs. (B1)–(B4) with a suitable subscript
g: statistical weight
h: Planck's constant (J s)
H: Heaviside function
I': dimensional current (A)
I: nondimensional current ($= I'/I_R'$)
I_R': normalization current (A)
k: Boltzmann constant (J/K); iteration parameter for number densities
L: gap length on the discharge axis (m)
l: present time level t (values of all the primitive dependent variables are known)
$l+1$: future time level, $t+\Delta t$ (values of all the primitive dependent variables are unknown)
N: dimensional number density (m^{-3})
N_R: number density used in normalizing the charged particle densities (m^{-3}) [$=kT_\infty\epsilon_0/(e^2d^2)$]
n: nondimensional number density (appropriately subscripted) ($=N/N_R$)
P: volumetric production terms (m^{-3}/s)
R: volumetric recombination terms (m^{-3}/s)
p: pressure (Pa)
T': dimensional temperature (K)
T: dimensionless temperature ($= T'/T_\infty'$)
t': dimensional time (s)
t: nondimensional time ($= t'/t_R'$)
t_R': time used in normalization (s) [$= 1/(A_i p\mu_e E_R')$]
Δt: time step
u,v,ϕ: prolate spheroidal coordinates
V: dimensional electrostatic potential (V)
x,y,z: Cartesian coordinates.

Greek symbols

ϵ_0: permittivity of free space (F/m)
ψ: dimensionless potential ($= eV/kT_\infty'$)
Γ: particle current density ($m^{-2}\,s^{-1}$)
μ: mobility of a charged particle in an electric field (m^2/V s).

Superscripts

$'$: dimensional quantity
$-$: negative-ion species.

Subscripts

ad: dissociative attachment
ct: charge transfer
d: detachment
e: electrons
i: impact ionization
n: neutral particles
O^- negative ions of atomic oxygen
O_2^- negative ions of molecular oxygen
0: initial values ($t'=0$); threshhold value
R: reference quantities
w: wire
$+$: positive ions
∞: ambient.

APPENDIX B: NONDIMENSIONAL FORM OF GOVERNING EQUATIONS

(1) Positive-ion conservation equation:

$$\frac{\partial n_+}{\partial t}-\frac{F_+}{\sinh^2 u+\sin^2 v}\left[\frac{1}{\sinh u}\frac{\partial}{\partial u}\left(\sinh u\, n_+\frac{\partial\psi}{\partial u}\right)+\frac{1}{\sin v}\frac{\partial}{\partial v}\left(\sin v\, n_+\frac{\partial\psi}{\partial v}\right)\right]$$
$$=\frac{F_+T_+}{\sinh^2 u+\sin^2 v}\left[\frac{1}{\sinh u}\frac{\partial}{\partial u}\left(\sinh u\frac{\partial n_+}{\partial u}\right)+\frac{1}{\sin v}\frac{\partial}{\partial v}\left(\sin v\frac{\partial n_+}{\partial v}\right)\right]+e^{-B_i/E}n_eE+C_1C_2n_eT_e^{-3}e^{-\psi_i/T_e}-C_1T_e^{-9/2}n_e^2n_+. \tag{B1}$$

(2) Electron conservation equation:

$$\frac{\partial n_e}{\partial t}+\frac{F_e}{\sinh^2 u+\sin^2 v}\left[\frac{1}{\sinh u}\frac{\partial}{\partial u}\left(\sinh u\, n_e\frac{\partial\psi}{\partial u}\right)+\frac{1}{\sin v}\frac{\partial}{\partial v}\left(\sin v\, n_e\frac{\partial\psi}{\partial v}\right)\right]$$
$$=\frac{F_eT_e}{\sinh^2 u+\sin^2 v}\left[\frac{1}{\sinh u}\frac{\partial}{\partial u}\left(\sinh u\frac{\partial n_e}{\partial u}\right)+\frac{1}{\sin v}\frac{\partial}{\partial v}\left(\sin v\frac{\partial n_e}{\partial v}\right)\right]+e^{-B_i/E}n_eE+C_1C_2n_eT_e^{-3}e^{-\psi_i/T_e}-C_1T_e^{-9/2}n_e^2n_+$$
$$-A_{ad}n_eE+A_d\left(\frac{\mu_{O^-}}{\mu_e}\right)e^{-B_d/E}n_{O^-}E. \tag{B2}$$

(3) O^- conservation equation:

$$\frac{\partial n_{O^-}}{\partial t}+\frac{F_{O^-}}{\sinh^2 u+\sin^2 v}\left[\frac{1}{\sinh u}\frac{\partial}{\partial u}\left(\sinh u\, n_{O^-}\frac{\partial\psi}{\partial u}\right)+\frac{1}{\sin v}\frac{\partial}{\partial v}\left(\sin v\, n_{O^-}\frac{\partial\psi}{\partial v}\right)\right]$$
$$=\frac{F_{O^-}T_{O^-}}{\sinh^2 u+\sin^2 v}\left[\frac{1}{\sinh u}\frac{\partial}{\partial u}\left(\sinh u\frac{\partial n_{O^-}}{\partial u}\right)+\frac{1}{\sin v}\frac{\partial}{\partial v}\left(\sin v\frac{\partial n_{O^-}}{\partial v}\right)\right]+A_{ad}n_eE-\left(\frac{\mu_{O^-}}{\mu_e}\right)A_de^{-B_d/E}n_{O^-}E-\left(\frac{\mu_{O^-}}{\mu_e}\right)$$
$$\times A_{ct}(E-E_{0,ct})H(E-E_{0,ct})n_{O^-}E. \tag{B3}$$

(4) O_2^- conservation equation:

$$\frac{\partial n_{O_2^-}}{\partial t}+\frac{F_{O_2^-}}{(\sinh^2 u+\sin^2 v)}\left[\frac{1}{\sinh u}\frac{\partial}{\partial u}\left(\sinh u\, n_{O_2^-}\frac{\partial\psi}{\partial u}\right)+\frac{1}{\sin v}\frac{\partial}{\partial v}\left(\sin v\, n_{O_2^-}\frac{\partial\psi}{\partial v}\right)\right]$$
$$=\frac{F_{O_2^-}T_{O_2^-}}{\sinh^2 u+\sin^2 v}\left[\frac{1}{\sinh u}\frac{\partial}{\partial u}\left(\sinh u\frac{\partial n_{O_2^-}}{\partial u}\right)+\frac{1}{\sin v}\frac{\partial}{\partial v}\left(\sin v\frac{\partial n_{O_2^-}}{\partial v}\right)\right]+\left(\frac{\mu_{O_2^-}}{\mu_e}\right)A_{ct}(E-E_{0,ct})H(E-E_{0,ct})n_{O^-}E. \tag{B4}$$

(5) Electrostatic potential:

$$\frac{1}{\sinh^2 u+\sin^2 v}\left[\frac{1}{\sinh u}\frac{\partial}{\partial u}\left(\sinh u\frac{\partial\psi}{\partial u}\right)+\frac{1}{\sin v}\frac{\partial}{\partial v}\left(\sin v\frac{\partial\psi}{\partial v}\right)\right]=\frac{a^2}{d^2}(n_e+n_{O^-}+n_{O_2^-}-n_+). \tag{B5}$$

[1] F. Llewellyn-Jones, *Ionization and Breakdown in Gases* (Methuen, London, 1957).
[2] J. Dutton, in *Electrical Breakdown in Gases*, edited by J. M. Meek and J. D. Craggs, (Wiley, New York, 1978), Chap. 3, p. 209.
[3] E. E. Kunhardt, IEEE Trans. Plasma Sci. **PS-8**, 130 (1980).
[4] H. Raether, *Electron Avalanches and Breakdown in Gases* (Butterworths, London, 1964).
[5] L. B. Loeb, *Electrical Coronas—Their Basic Physical Mechanisms* (University of California Press, Berkeley, CA, 1965).
[6] A. J. Davies, Proc. IEE **133** (Pt. A), 217 (1986).
[7] A. J. Davies, C. J. Evans, and P. Townsend, Proc. IEE **124**, 179 (1977).
[8] K. Yoshida and H. Tagashira, J. Phys. D **9**, 435 (1976).
[9] J. P. Novak and R. Bartnikas, J. Appl. Phys. **62**, 3605 (1987).
[10] F. Bastien and E. Marode, J. Phys. D **18**, 377 (1985).
[11] R. Morrow, Phys. Rev. A **32**, 1799 (1985).
[12] K. Ramakrishna, I. M. Cohen, and, P. S. Ayyaswamy, J. Appl. Phys. **65**, 41 (1989).
[13] K. Ramakrishna, Ph.D. dissertation, University of Pennsylvania, PA (1989).
[14] K. G. Donovan and I. M. Cohen, J. Appl. Phys. **70**, 4132 (1991).
[15] M. A. Jog, I. M. Cohen, and P. S. Ayyaswamy, Phys. Fluids B **3**, 3532 (1991).
[16] M. A. Jog, I. M. Cohen, and P. S. Ayyaswamy, Phys. Fluids B **4**, 465 (1992).
[17] D. J. Vacek and I. M. Cohen, J. Appl. Phys. **65**, 1005 (1989).
[18] R. S. Sigmond, in *Electrical Breakdown in Gases*, edited by J. M. Meek and J. D. Craggs (Wiley, New York, 1978), Chap. 4, p. 319.
[19] R. T. Waters, in *Electrical Breakdown in Gases*, edited by J. M. Meek and J. D. Craggs (Wiley, New York, 1978), Chap. 5, p. 385.
[20] R. T. Waters, Proc. IEE **128** (Pt. A), 319 (1981).
[21] M. Goldman and R. S. Sigmond, IEEE Trans. Electr. Insul. **EI-17**, 90 (1982).
[22] P. Bayle and M. Bayle, Z. Phys. **266**, 275 (1974).
[23] L. E. Kline, J. Appl. Phys. **46**, 1994 (1975).
[24] J. Dutton, J. Phys. Chem. Ref. Data **4**, 577 (1975).
[25] J. W. Gallagher, E. C. Beaty, J. Dutton, and L. C. Pitchford, J. Phys. Chem. Ref. Data **12**, 109 (1983).
[26] J. L. Moruzzi and A. V. Phelps, J. Chem. Phys. **45**, 4617 (1966).

[27]W. P. Allis, in *Handbuch der Physik*, edited by S. Flügge (Springer-Verlag, Berlin, 1956), Vol. XXI.
[28]D. R. Wilkins and E. P. Gyftopoulos, J. Appl. Phys. **37**, 3533 (1966).
[29]N. Lebedev, *Special Functions and their Applications*, translated by R. A. Silverman (Dover, New York, 1972).
[30]R. G. Fleagle and J. A. Businger, *An Introduction to Atmospheric Physics* 2nd ed. (Academic, New York, 1980), Vol. 25, pp. 135 and 150.
[31]A. N. Prasad, Proc. Phys. Soc. London **74**, 33 (1959).
[32]M. A. Harrison and R. Geballe, Phys. Rev. **91**, 1 (1953).
[33]A. N. Prasad and J. D. Craggs, Proc. Phys. Soc. London **77**, 385 (1961).
[34]N. Sukhum, A. N. Prasad, and, J. D. Craggs, Br. J. Appl. Phys. Ser. 2, **18**, 785 (1967).
[35]M. J. Eccles and J. D. Craggs, Electron. Lett. **3** (4), 146 (1967).
[36]T. N. Daniel, J. Dutton, and, F. M. Harris, Br. J. Appl. Phys. Ser. 2 **2**, 1559 (1969).
[37]K. H. Wagner, Z. Phys. **241**, 258 (1971).
[38]J. L. Moruzzi and D. A. Price, J. Phys. D **7**, 1434 (1974).
[39]J. Dutton, F. Llewellyn-Jones, and R. W. Palmer, Proc. Phys. Soc. London **78**, 569 (1961).
[40]S. C. Brown, *Basic Data of Plasma Physics, 1966*, 2nd revised ed. (MIT Press, Cambridge, MA, 1967), p. 126.
[41]K. Ramakrishna, I. M. Cohen, and, P. S. Ayyaswamy, J. Comput. Phys. **104**, 173 (1993).
[42]S. V. Patankar, *Numerical Heat Transfer and Fluid Flow* (Hemisphere, Washington, DC, 1980).